Stochastic Dynamics in Irreversible Nonequilibrium Environments. 3. Temperature-Ramped Chemical Kinetics

Frank L. Somer, Jr.[†] and Rigoberto Hernandez*

School of Chemistry and Biochemistry, Georgia Institute of Technology, Atlanta, Georgia 30332-0400

Received: May 14, 1999; In Final Form: August 16, 1999

A generalization of the generalized Langevin equation (stochastic dynamics) is introduced in order to model chemical reactions which take place in environments with both density and temperature variations. This phenomenological construction—given the name irreversible generalized Langevin equation (iGLE)—ensures that both the bath and its response to the chosen coordinates of the projected systems are characterized by the same imposed temperature profile. As in the earlier construction, the present generalization does reproduce the generalized Langevin equation in equilibrium and quasi-equilibrium limits. Numerical results indicate surprising behavior when the temperature ramping conditions are fast compared to the solvent response.

I. Introduction

Understanding the dynamics of chemical reactions is a primary objective of theoretical chemistry. For those reactions which have an easily identifiable reaction coordinate coupled to the solvent through a uniform response, this understanding is fairly complete.[1−9] In these cases, the dynamics of an effective one-dimensional, or few−dimensional, subsystem are well described by a projection of the equations of motion of a full-dimensional mechanical system. The projected equations of motion, called the generalized Langevin equation (GLE), involve an effective potential of mean force (PMF) and associated stochastic forces.[1,10−18] A new level of difficulty arises, however, if the solvent response is no longer stationary. The nonstationarity is presumably due to an *irreversible* variation, in the volume or temperature, for example, of the solvent, which is dissimilar to the irreversibility in the subsystem that is already considered within the GLE. In the present series,[19,20] we have constructed a new class of stochastic equations of motion involving nonstationary friction kernels that thereby include this additional irreversible phenomenon, and have named it the irreversible generalized Langevin equation (iGLE).

The iGLE represents our initial attempt at formulating a consistent nonstationary stochastic theory to describe the dynamics of the reduced-dimensional subsystem vis-a-vis the chosen coordinates. Since the seminal work of Andersen,[21] several groups have described the construction of static and dynamic averages for a variety of ensembles.[22−26] This effort allows for the construction of full-dimensional molecular dynamics with fluctuating volume in constant-pressure ensembles, and fluctuating energy in the canonical ensemble, for example. Presumably, irreversible variations in these variables which are sufficiently slow—adiabatic—that linear response theory is valid may also be characterized with these approaches. However, for faster irreversible variations this is not necessarily so, and a new theory is needed. It is the projection of such a theory with respect to the reduced-dimensional subsystem that is the object of this work. The iGLE has been suggested as a candidate stochastic equation of motion to describe systems with irreversible volume variations, not just fluctuations, and has been shown to be phenomenologically consistent with various desired limits.[19] In concurrent work, we have also shown that it is the projection of an open Hamiltonian system where the irreversibility in the volume variations is indirectly described by an irreversible parameter controlling the degree to which the bath is confined.[27]

In summary, the specific irreversibility addressed in the previous work of this series involves variations in the friction at constant temperature.[19,20,27] While this case is of interest in describing, for example, the dynamics of a tagged particle in an environment which is undergoing an isothermal compression, its generalization to include irreversible temperature variations would enable a variety of new applications of the theory. A particularly important example of such an application would be the consideration of temperature-ramped chemical kinetics. Other variable-temperature applications might include thermostating in molecular-dynamics (MD) simulations,[28] nonequilibrium simulations of colloidal suspensions,[28,30] and simulations of adsorbed systems where the boundary layer of the effective microscopic box is coupled to a stochastic heat bath with the other layers being governed by deterministic MD.[28,32]

In the present paper, we will further generalize the iGLE to describe irreversible temperature variations. After giving a brief review of the constant-temperature iGLE (section II), we introduce in section III a method for allowing temporal variations in the temperature of the heat bath. This method takes advantage of the properties of Gaussian random processes (as outlined in the Appendix) to allow us to vary the bath temperature on arbitrary time scales while still obtaining the correct limiting behavior at equilibrium. The resulting iGLE formalism is shown to satisfy a generalized, nonstationary version of the fluctuation−dissipation theorem. An important feature of this method is that it leads to much more accurate tracking of a rapidly varying temperature bath, where the effective temperature is determined through the mean-square random force (MSRF), than does the naive (albeit adiabatically correct) alternative method of varying the temperature in the auxiliary Gaussian bath. This advantage and some consequences

* Author to whom correspondence should be addressed. E-mail: hernandez@chemistry.gatech.edu.

[†] Current address: Department of Chemistry, St. John's University, 8000 Utopia Pkwy., Jamaica, NY 11430.

10.1021/jp9915836 CCC: $18.00
Published on Web 11/24/1999

thereof are illustrated in section IV by way of numerical simulations using several different temperature profiles and friction-kernel decay times. We find that the system properties, e.g. the instantaneous system temperature determined through the mean-square velocity (MSV), obtained from the new iGLE are generally more responsive to temperature variations than those obtained from the naive adiabatic method. The iGLE also shows qualitative structure in the time evolution that the adiabatic method fails to produce.

II. Constant-Temperature iGLE

The dynamics of the iGLE may be characterized by the stochastic differential equation,

$$\dot{v}(t) = -\int^t \mathrm{d}t'\, g(t)g(t')\gamma_0(t-t')v(t') + g(t)\xi_0(t) + F(t) \quad (1)$$

where $F(t)$ ($\equiv -\nabla_q V(q(t))$) is the external force, v ($=\dot{q}$) is the velocity, and q is the mass-weighted position. The random force $\xi_0(t)$ due to the solvent is related to the stationary friction kernel $\gamma_0(t,t')$ through the fluctuation−dissipation (FD) theorem[33]

$$\langle \xi_0(t)\cdot\xi_0(t')\rangle = k_B T_0 \gamma_0(t-t') \quad (2)$$

where T_0 is some fixed temperature and is usually set to the initial temperature in the infinite past. The function $g(t)$ characterizes the irreversible change in the solvent response. It is required to go to a constant at infinite time, so that the iGLE will go to an equilibrium GLE at long times.

By construction, the generalized random force

$$\xi(t) \equiv g(t)\xi_0(t) \quad (3)$$

in eq 1 satisfies a nonstationary version of the FD relation

$$\langle \xi(t)\cdot\xi(t')\rangle = k_B T_0 \gamma(t,t') \quad (4a)$$

$$\equiv k_B T_0 g(t)g(t')\gamma_0(t-t') \quad (4b)$$

where the nonstationary friction kernel, $\gamma(t,t')$, has been implicitly defined. In the $t = t'$ limit, one obtains the time-dependent MSRF

$$\langle \xi^2(t)\rangle = k_B T_0 g^2(t)\gamma_0(0) \quad (5)$$

We have shown that the iGLE, interpreted as a nonstationary ("irreversible") GLE, gives the correct equilibrium behavior in quasi-equilibrium limits and in illustrative models.[19,20] In the case that g represents a change in the solvent response due to outside forces, we have thus far explored the iGLE with constant and biased potentials. The form of g has been taken as a switching function which changes the solvent from a lower to a higher effective friction constant, $g^2(t)\gamma_0$. The results show that the iGLE dynamics does satisfy equipartition well beyond the equilibrium limit.

III. Stochastic Dynamics with Temperature Variation

A. Naive Adiabatic Temperature Variation. Perhaps the most straightforward way to introduce irreversible temperature variations in the iGLE formalism is to simply replace the temperature T_0 (which appears in the auxiliary dynamics for the random force ξ_0) with a time-dependent profile $\theta(t)$. For example, if (as in the numerical simulations of refs 19 and 20, as well as those presented later in the present paper), we take the stationary part of the friction kernel to have the exponential form[34−37]

$$\gamma_0(t-t') = \gamma_0(0)\, \mathrm{e}^{-|t-t'|/\tau} \quad (6)$$

and generate the random force via the auxiliary Langevin equation,

$$\dot{\xi}_0(t) = -(1/\tau)\xi_0(t) + \xi_G(t) \quad (7)$$

then the uncorrelated Gaussian random force ξ_G would have the variance

$$\langle \xi_G{}^2(t)\rangle = \gamma_G = 2\gamma_0(0)k_B\theta(t)/\tau \quad (8)$$

That is, at a given time t in a given realization, $\xi_G(t)$ is a random number chosen from the Gaussian distribution with the variance of eq 8. (We use the term "naive" to describe this choice of ξ_G to impose the temperature constraint because it constrains the auxiliary Gaussian bath rather than the bath itself.)

Consequently, in regimes where $\theta(T)$ varies rapidly compared to τ, the variance of the induced random force $\xi_0(t)$, will *not* satisfy an instantaneous FDR

$$\langle \xi_0{}^2(t)\rangle = k_B T \gamma_0(0) \quad (9)$$

Alternatively, when $\theta(t)$ is constant or slowly varying compared to τ, the inhomogeneity in eq 7 will decay away, and so the instantaneous FDR of eq 9 will be satisfied. In this latter limit, the imposed temperature on the bath, vis-a-vis $\xi_G(t)$, is the same as the temperature in the response of the bath to the chosen coordinate. Since this condition is satisfied only for slow temperature variations, the use of the equations of this subsection to control temperature variations will be called the *naive adiabatic* approach throughout this paper.

While this intuitively attractive procedure should be satisfactory for adiabatic temperature variations as noted above, it may not be satisfactory for irreversible temperature variations in which the heat bath, represented by the random force, will not be in "temperature equilibrium"; i.e. eq 2 and therefore eq 4b, with T replaced by $\theta(t)$, will generally not be satisfied. Thus, analysis of the resulting iGLE is complicated by having two simultaneous nonequilibrium processes each characterized by a different effective temperature: one due to the response of the auxiliary dynamics to the irreversible temperature variation in an arbitrary Gaussian bath vis-a-vis ξ_G, and another due to the response of the chosen coordinate to the resulting nonequilibrium random force. Neither does this method suggest an obvious extension to the FD relation, which might otherwise have brought some conceptual order to this situation.

B. Temperature Variation in the iGLE. An alternative procedure for introducing irreversible temperature variations would be to run the auxiliary dynamics at the *constant* temperature T_0 and then rescale the resulting random force by a factor of $\sqrt{\theta(t)/T_0}$. As detailed in the Appendix, in the constant-temperature equilibria before and after a temperature variation, this alternative approach is effectively identical to the above intuitive procedure. During an irreversible temperature variation, however, it is superior in that it guarantees the instantaneous temperature equilibrium, i.e., eq 5, of the heat bath, regardless of the temperature profile used, and leads to a natural extension of the FD relation.

Specifically, the iGLE random force of eq 3 is redefined

$$\xi(t) \equiv \sqrt{\frac{\theta(t)}{T_0}}\, g(t)\xi_0(t) \quad (10)$$

where $\theta(t)$ is a time-dependent temperature profile and T_0 is

the constant temperature at which we run the auxiliary dynamics. This leads to a revised FD relation

$$\langle \xi(t)\xi(t')\rangle = k_B\sqrt{\theta(t)\theta(t')}g(t)g(t')\gamma_0(t-t') \quad (11a)$$

$$\equiv k_B\sqrt{\theta(t)\theta(t')}\gamma(t,t') \quad (11b)$$

which is appealing because (i) in time regimes where $\theta(t)$ is approximately constant relative to the the decay time of γ, it reduces to the usual thermalized FD relation; and (ii) it satisfies the instantaneous FDR of eq 9. Thus, this generalization of the iGLE to include temperature variations satisfies the corresponding equipartition theorem in the equilibrium limit.

C. Quasi-equilibrium Limit of the iGLE. As in the initial paper on the iGLE,[19] we can write the variable-temperature iGLE in frequency space as

$$i\omega v(\omega) = \int_{-\infty}^{\infty} d\omega_1 \int_{-\infty}^{\infty} d\omega_2\, \theta(\omega_2)g(\omega-\omega_1)\xi_0(\omega_1) - \int_{-\infty}^{\infty} d\omega_1 \int_{-\infty}^{\infty} d\omega_2\, g(\omega-\omega_1)\gamma_0[\omega_1]g(\omega_1-\omega_2)v(\omega_2) \quad (12)$$

where $g(\omega)$ and $\theta(\omega)$ are the Fourier transforms of $g(t)$ and $\theta(t)$, respectively. As before, we assume that in quasi-equilibrium regimes, under quasi-adiabatic temperature variations, there exists a characteristic time $\bar{t}$ such that

$$\tilde{g}(\omega) \approx g(\bar{t})\delta(\omega) \quad (13a)$$

$$\tilde{\theta}(\omega) \approx \theta(\bar{t})\delta(\omega) \quad (13b)$$

where the tilde on the variables denotes the local Fourier transform

$$\tilde{f}(\omega) \equiv (1/2\pi)\int_{\bar{t}-\delta}^{\bar{t}+\delta} dt\, e^{-i\omega t} f(t) \quad (14)$$

which reverts to the Fourier transform in the limit that δ goes to infinity. Use of eqs 13 in a locally transformed version of eq 12 leads to

$$i\omega\tilde{v}(\omega) = -g(\bar{t})^2\gamma_0[\omega]\tilde{v}(\omega) + \theta(\bar{t})g(\bar{t})\tilde{\xi}_0(\omega) \quad (15)$$

Following the analysis from eqs 16−21 in ref 19, we obtain

$$\langle v^2\rangle = \theta(\bar{t}) \quad (16)$$

which is precisely the form of the desired adiabatic equipartition theorem.

The extension of the iGLE to include temperature variations gives the correct behavior in equilibrium and quasi-equilibrium regimes. It also ensures the instantaneous equilibrium of the random-force distribution (viz. the heat bath) and consequently unifies the irreversible nature of the iGLE into a single form. Thus, the temperature-ramping scheme provided through eq 10 constitutes a reasonable and practical generalization of the iGLE to include irreversible temperature variations.

IV. Numerical Simulations

We now explore and contrast the characteristics of the naive adiabatic approach and the iGLE method for temperature-ramped chemical kinetics. In order to limit the analysis to that of temperature variations only, the nonstationarity component $g(t)$ is set to unity. The stationary part of the friction kernel is taken to be of the exponential form in eq 6.[34−37] The following parameters are common to all the simulations presented herein: $N = 10\,000$, $\gamma_0(0) = 10.0$, $\Delta t = 4.0 \times 10^{-3}$, and $\Delta t_\xi = 4.0 \times 10^{-4}$, all in reduced units. (Recall that N is the number of trajectories—realizations—to be averaged over, Δt is the time step for the iGLE dynamics, and Δt_ξ is the time step for the auxiliary dynamics of the associated Langevin equation, eq 7.) A discussion of the technical details of the integration is given in ref 19; no additional complications arise as a result of the inclusion of temperature variations.

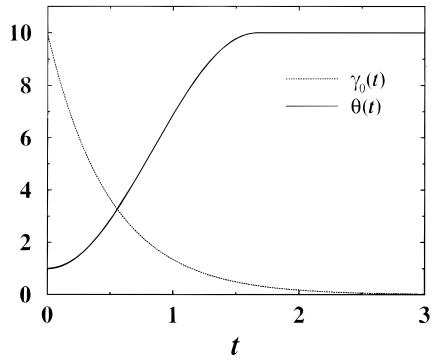

Figure 1. Stationary friction kernel γ_0 (dotted curve) and the "switching-function" temperature profile θ (solid curve) as a function of time. The parameters used are $\theta_1 = 1$, $\theta_2 = 10$, $\tau_\theta = 1.66$, and $\tau = 0.5$. (The quantities plotted here have different dimensions but are shown on the same graph for ease of comparison; this also applies to Figures 4, 5, 6, and 7.)

In what follows, we will explore a series of numerical experiments in which the naive adiabatic GLE and the iGLE are used to obtain the response of the chosen coordinates to various fast temperature changes in the bath. By "fast," we mean that the change in the temperature of the bath modes is faster than the solvent response time. As such, the heating and cooling of the bath modes cannot be due only to surface effects. Instead, all the bath modes must be heated or cooled simultaneously and at a faster time scale than their response time. This can be accomplished with laser pulses that excite the vibrational modes of each of the bath modes and for which the intramolecular vibrational energy relaxation between the bath modes is faster than the response time, τ, of the bath modes to the motion of the chosen—projected—coordinate. (Such a separation of time scales is certainly observable in glassy dynamics and may be seen in certain liquids, as well.) A conceptually simple and interesting experiment, discussed in section IVC, involves subjecting the sample to a train of laser pulses used to cycle the bath between two different temperatures. The switching function, or half-pulse, and full pulse discussed in section IV, parts A and B, may also be experimentally realizable, but are included primarily to help analyze the various effects in the pulse train.

A. "Switching-Function" Temperature Profile. We first consider the response of the system to a simple, monotonic change from one temperature to another. The specific profile used is that of two constant-temperature limits joined smoothly through the form

$$\theta(t) \equiv \begin{cases} \theta_1 & \text{for } t < 0 \\ {}^1/_2(\theta_2-\theta_1)[1-\cos(\pi t/\tau_\theta)] + \theta_1 & \text{for } 0 < t < \tau_\theta \\ \theta_2 & \text{for } t > \tau_\theta \end{cases} \quad (17)$$

where τ_θ is the turn-on time. The temperature profile and the friction kernel displayed in Figure 1 have parameters chosen such that there is a significant temperature variation and the time scales of the variation and the response are comparable. If the response is fast compared to the time scale of the temperature variation, the iGLE recovers the adiabatic result of section IIIA.

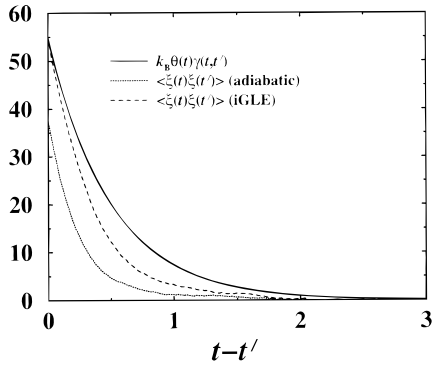

Figure 2. Comparison of the random-force correlation functions observed in the adiabatic (dotted curve) and iGLE (dashed curve) methods and the nonstationary friction kernel (solid curve) as a function of $(t - t')$, and at the intermediate time $\tau_\theta/2$ (=0.83). The temperature-ramping conditions are those of Figure 1.

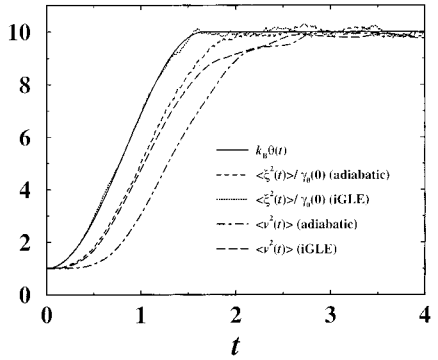

Figure 3. Comparison of the temperature profile $k_B\theta(t)$ (solid curve), the mean-square random force $\langle\xi^2(t)\rangle$ (divided by $\gamma_0(0)$(=10.0) in order to fit the scale of the plot), and the mean-square velocity $\langle v^2(t)\rangle$ for each method, as a function of time. The adiabatic MSRF, iGLE MSRF, adiabatic MSV, and iGLE MSV, are displayed by short-dashed, dotted, dot-dashed, and long-dashed curves, respectively.

The time correlation functions of the random force, $\langle\xi(t)\xi(t')\rangle$, (with parameters as in Figure 1) for both methods are displayed in Figure 2. Also displayed is the reference function $k_B\theta(t)\gamma(t,t')$ which, for constant (or adiabatically varying) temperature, is equal to $\langle\xi(t)\xi(t')\rangle$. The fact that the three curves are clearly different indicates the irreversibility of the temperature variation. Note, however, that as required by eq 11 the *intercept* of the correlation function (i.e., the MSRF) is equal to that of the reference function for the iGLE, but not for the adiabatic method. This graphically demonstrates that the iGLE maintains the instantaneous temperature equilibrium of the heat bath, while the adiabatic method fails to do so for fast temperature variations.

The MSRF (normalized by $\gamma_0(0)$ in order to fit the scale of the plot) and mean-square velocity (MSV) for both methods are compared to the temperature profile in Figure 3. Once again, for a reversible transformation (and for $N \rightarrow \infty$, where fluctuations are negligible) all five curves would be identical. As noted above, the iGLE is constructed such that $\langle\xi^2(t)\rangle/\gamma_0(0)$ follows the imposed temperature precisely, regardless of its rate of change, as is confirmed in the figure to within finite-size fluctuations. This leads to a MSV (effectively the temperature of the *system*, as opposed to the bath) that is much more responsive to temperature variations in the bath than that obtained from the naive method. As seen in Figure 3, the response of the system is made unduly sluggish because it is driven by a random force which lags behind the correct value corresponding to the current value of the temperature profile.

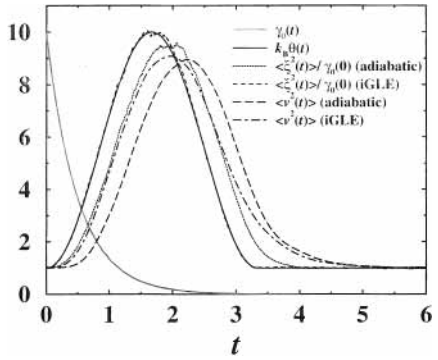

Figure 4. A comparison of the MSRF's and MSV's obtained in the adiabatic and iGLE methods for the case in which the time scale, $\tau = 0.5$, of the friction kernel, $\gamma_0(t)$ (solid gray line), is much faster than the ramping time, $\tau_\theta = 1.66$, in the temperature profile, $\theta(t)$ (solid black line). The remaining curves are as in Figure 3.

B. Pulsed Temperature Profile. To further probe the variable-temperature behavior of the iGLE, we now consider hysteresis effects. The temperature profiles take the system smoothly but quickly (with time scale τ_θ) from an initial temperature θ_1 to a higher temperature θ_2, maintain θ_2 for a delay time τ_d, and finally return the system smoothly to θ_1. Specifically, $\theta(t)$ is defined through the form

$$\theta(t) - \theta_1 \equiv \begin{cases} 0 & \text{for } t < 0 \\ {}^1/_2(\theta_2 - \theta_1)[1 - \cos(\pi t/\tau_\theta)] & \text{for } 0 \le t < \tau_\theta \\ \theta_2 - \theta_1 & \text{for } \tau_\theta \le t < \tau_{\theta,d} \\ {}^1/_2(\theta_2 - \theta_1)[1 - \cos(\pi(t - \tau_d)/\tau_\theta)] & \text{for } \tau_{\theta,d} \le t < \tau_{2\theta,d} \\ 0 & \text{for } \tau_{2\theta,d} \le t \end{cases} \tag{18}$$

where $\tau_{\theta,d} \equiv \tau_\theta + \tau_d$, and $\tau_{2\theta,d} \equiv 2\tau_\theta + \tau_d$.

Using the same parameters as in Figure 1 with $\tau_d = 0$ to obtain a single temperature pulse, we find the behavior displayed in Figure 4. As before, the friction kernel and temperature profile have similar time scales, and we find the qualitative behavior we would expect based on the previous results. The MSRF in the iGLE follows the temperature profile reversibly, while that from the naive method lags behind, which, owing to the peaked form of θ, causes $\langle\xi^2(t)\rangle$ to peak below its reference (reversible) value. The MSV's behave accordingly: the curve for the naive method lagging behind that of the iGLE and peaking later at a lower value. If we increase the time scale ratio of the friction kernel to the temperature profile by taking $\tau = 1.0$ and $\tau_\theta = 0.83$, as seen in Figure 5, the MSRF's are qualitatively similar to those seen in the previous case. The hysteresis associated with the naive method simply becomes more pronounced. The MSV in the iGLE is, however, dramatically different from that of Figure 4, exhibiting structure (at least five clear maxima) beyond the simple peaked form of $\theta(t)$. The MSV in the naive method also shows some additional structure, but this is much more muted, still displaying only a single maximum.

This change in behavior of the MSV is clearly a memory effect, and to further examine this connection, we now consider the effect of a nonzero plateau, τ_d, at the higher temperature. In Figure 6 we show the MSV's obtained for $\tau = 1.0$ and $\tau_\theta = 0.83$ as in Figure 5, and with three different values of τ_d. Even for the very small plateau $\tau_d = 0.25$, the structure of the MSV in the iGLE is significantly softened. The naive method, being less responsive, gives a MSV which is relatively unchanged

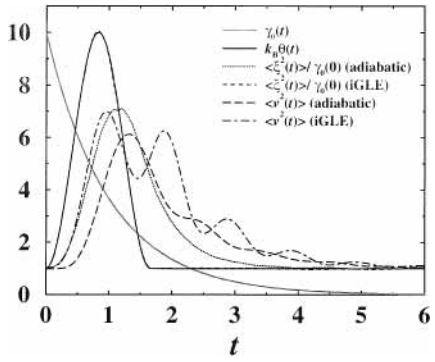

Figure 5. A comparison of the MSRF's and MSV's obtained in the adiabatic and iGLE methods as in Figure 4, but with $\gamma_0(t)$ having a much slower time scale, τ =1.0, than the ramping time, $\tau_\theta = 0.83$, in $\theta(t)$.

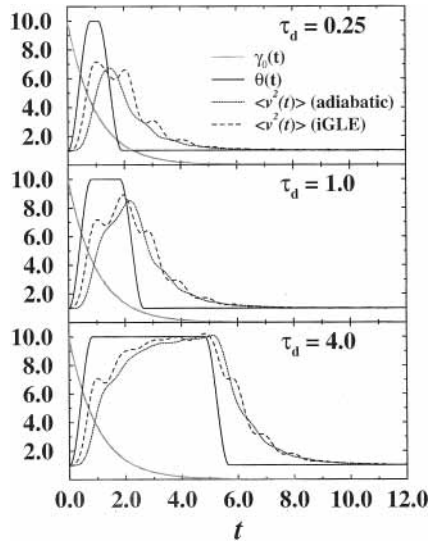

Figure 6. A comparison of the MSV's obtained in the adiabatic and iGLE methods, for pulsed temperature profiles whose turn-on time, $\tau_\theta = 0.83$, and friction response time, $\tau = 1.0$ as in Figure 5, for various delay times, $\tau_d = 0.25$, 1.0, and 4.0. The friction kernel $\gamma_0(t)$, temperature ramp, adiabatic MSV, and iGLE MSV are displayed by solid gray, solid, dotted, and short-dashed curves, respectively.

from the simple pulsed case. These trends continue for increasing τ_d until we reach the point where the friction kernel decays to a very small value within the span of the plateau, as seen for $\tau_d = 4.0$. In this case, the MSV obtained while heating becomes uncorrelated with that obtained while cooling. Any further increase in τ_d leaves the structure of the MSV unchanged except for the increased time spent at $\langle v^2(t)\rangle = \theta_2$. Nevertheless, there remains some structure in the MSV due to the sudden change in θ at the edges of the plateau.

C. Oscillatory Temperature Profile. Finally, we consider the case of a temperature profile which is initially fixed and then oscillates sinusoidally between θ_1 and θ_2 for $t \geq 0$:

$$\theta(t) \equiv \begin{cases} \theta_1 & \text{for } t < 0 \\ \frac{1}{2}(\theta_2 - \theta_1)[1 - \cos(\pi t/\tau_\theta)] + \theta_1 & \text{for } t > 0 \end{cases} \quad (19)$$

Once again taking $\theta_1 = 1$, $\theta_2 = 10$, and $\tau_\theta = 0.83$, we show in Figure 7 the MSRF for three different values of τ. As τ increases, the MSRF of the naive method lags further behind that of the iGLE, cycling with smaller and smaller amplitude. For $\tau = 2.0$, its amplitude is only about a fourth that of the reversible profile produced by the iGLE, highlighting the fact that the superiority

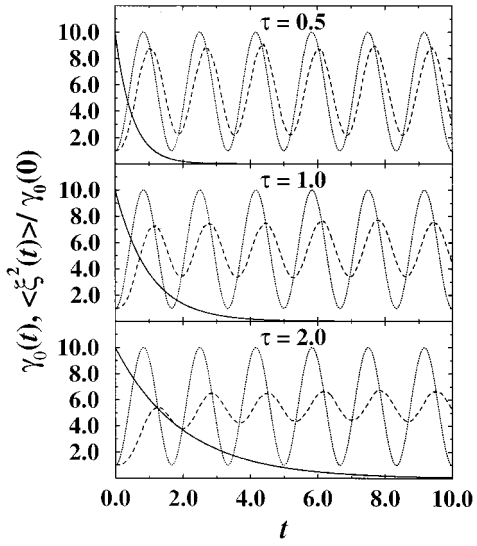

Figure 7. A comparison of the MSRF's obtained in the adiabatic and iGLE methods for oscillating temperature profiles (dotted curve) with period $2\tau_\theta = 1.66$, for various friction kernels (solid curve) as characterized by three different response times, $\tau = 0.5$, 1.0, and 2.0. The adiabatic MSRF is displayed by the short-dashed curve, while the iGLE MSRF matches the temperature profile (dotted curve) exactly.

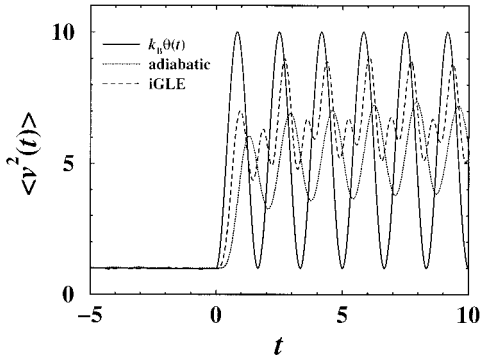

Figure 8. A comparison of the MSV's obtained in the adiabatic (dotted curve) and iGLE (short-dashed curve) methods, for the same oscillatory temperature profile (solid curve) used in Figure 7 with the response time $\tau = 1.0$ in $\gamma_0(t)$.

of the iGLE relative to the naive method increases with the length of the friction memory.

The resulting MSV's for the $\tau = 1.0$ case are displayed in Figure 8. As in the pulsed-temperature case of the previous section, the MSV obtained in the iGLE shows considerable structure (two peaks for every peak in θ) that the adiabatic method misses. Also note that the MSV in the iGLE appears to be shifted upward relative to that in the naive method. In fact, once both curves have settled into periodic behavior (after $t =$ 6, or so), the time average of the MSV in the iGLE is ~6.8, while the naive method gives an average of ~5.5, which is also the time average of θ. This difference is a result of the fact that (as seen most clearly in Figure 6) the iGLE responds much more quickly to heating than does the naive method, while both methods are similarly responsive to cooling. Thus, not only does the iGLE find detailed dynamics that the naive method misses, it can also give very different *time-averaged* properties in the presence of a cyclic temperature profile.

V. Concluding Remarks

The iGLE theory has been extended to include nonadiabatic variations in the temperature of the environment. As shown in section IV for a variety of temperature variations, the iGLE

provides instantaneous control of the bath temperature, even when a slowly decaying friction kernel (i.e., a long memory) necessitates that the random force be generated by intrinsically slow auxiliary dynamics. This differs from the naive adiabatic approach in which the bath has an implicit, and nonphysical, delay in its response to an imposed temperature variation. [Such a time delay might be expected in an experiment in which the bath was in turn heated or cooled by an even larger bath. However, the response time to such heating or cooling would be governed by a number of factors (such as the heating rate and the interaction strength between the bath and the larger bath) in which the bath relaxation time, τ, would only play a partial role. As such, the time delay in the naive adiabatic approach represents only the effects of heating or cooling due to the coupling of the bath to a (larger) artificial auxiliary Gaussian bath. The iGLE approach removes the time delay through a construction which ensures that the bath and its response are governed consistently by a single temperature.]

Interestingly, it was also found that the iGLE has a hysteresis effect, in that it responds more quickly to the "heating" phase of a pulsed (or cyclic) temperature profile than to the "cooling" phase. While this result may seem surprising on first inspection, it is actually a simple result of energy-diffusion-limited dynamics.[38] In this regime, there exists an activated rate process for the system to transfer between energy states. The rate is faster for higher temperature, and hence the system heats faster than it cools. A quantitative analysis of these diffusion rates and how they relate to the observed structure in the MSV will be the subject of future work.

Finally, it should be noted that the iGLE permits the study of stochastic dynamics on a reaction path coupled to a bath with externally controlled temperature variation, which should make it valuable in the study of temperature-ramped chemical kinetics.

Acknowledgment. We gratefully acknowledge John Tully for insightful discussions. This work has been partially supported by a National Science Foundation CAREER Award under Grant No. NSF 97-03372. R.H. is a Cottrell Scholar of the Research Corporation and Blanchard Assistant Professor of Chemistry at Georgia Tech.

Appendix: Role of Temperature in Gaussian Noise

The random force ξ_0 is generally taken to be Gaussian-distributed, colored noise. In what follows, we note some properties of Gaussian distributions which are useful in constructing the temperature-ramping scheme developed in Section III.

The odd moments of the distribution are all zero since it is symmetric about the origin. Defining the integral

$$I_n(\sigma) \equiv \int_{-\infty}^{\infty} x^n \, \mathrm{e}^{-x^2/2\sigma^2} \, \mathrm{d}x = \sqrt{2\pi}(n-1)!!\sigma^{n+1} \quad \text{(A1)}$$

where $(n-1)!! = 1\cdot3\cdot5...n-1$ and $0!! = -1!! = 1$, the even moments are given by

$$\langle x^n \rangle = I_n(\sigma)/I_0(\sigma) = (n-1)!!\sigma^n \quad \text{(A2)}$$

for n an even nonnegative integer. Interpreting the variable x as the stationary random force ξ_0, and recognizing that the FD theorem requires that we take the variance to be

$$\sigma^2 = \langle \xi_0{}^2 \rangle = k_B T_0 \gamma_0(0) \quad \text{(A3)}$$

the even moments of the stationary random-force distribution are

$$\langle \xi_0{}^n \rangle = (n-1)!![k_B\gamma(0)]^{n/2} \cdot T_0{}^{n/2} \quad \text{(A4)}$$

Thus, we see that the nth moment scales as the $(n/2)$th power of the temperature, i.e., the generic temperature variations $T_0 \rightarrow aT_0$ affects the moments per $\langle \xi_0{}^n \rangle \rightarrow a^{n/2}\langle \xi_0{}^n \rangle$.

It is also well-known[39] that a Gaussian deviate of variance σ^2 can be converted to one of variance σ'^2 by simply multiplying the latter deviate by σ'/σ. From eq A3 we see that in order to convert the random-force distribution from one appropriate to T_0 to one appropriate to temperature θ, we would multiply the random force, generated at T_0, by $\sigma_\theta{}^2/\sigma_{T_0}{}^2 = \sqrt{\theta/T_0}$, i.e.

$$\xi = \sqrt{\frac{\theta}{T_0}}\xi_0 \quad \text{(A5)}$$

which is identical to eq 10 with $g = 1$. Furthermore, in terms of eq A1 (once again identifying x with ξ_0), this transformation amounts to taking

$$\mathrm{I_n} \rightarrow \mathrm{I_n}' = \int_{-\infty}^{\infty} \left(\sqrt{\frac{\theta}{T_0}}x\right)^n \mathrm{e}^{-x^2/2\sigma^2} \, \mathrm{d}x = \left(\frac{\theta}{T_0}\right)^{n/2} I_n \quad \text{(A6)}$$

Using eqs A2 and A3, we find that

$$\langle \xi^n \rangle = (n-1)!![k_B\gamma(0)]^{n/2} \cdot \theta^{n/2}, \quad n = 0, 2, 4, ... \quad \text{(A7)}$$

which is the same as eq A4, with T_0 replaced by θ. This shows that for fixed-temperature θ, this procedure has exactly the same effect on the random force as does the previously discussed method of varying σ^2 directly. This is true not only for the variance but for *all* the moments of the distribution.

References and Notes

(1) Kramers, H. A. *Physica* **1940**, *7*, 284.
(2) Hynes, J. T. In *Theory of Chemical Reaction Dynamics*; Baer, M., Ed.; CRC: Boca Raton, FL, 1985; Vol. 4, p 171.
(3) Hynes, J. T. *Annu. Rev. Phys. Chem.* **1985**, *36*, 573.
(4) Nitzan, A. *Adv. Chem. Phys.* **1988**, *70*, 489.
(5) Berne, B. J.; Borkovec, M.; Straub, J. E. *J. Chem. Phys.* **1988**, *92*, 3711.
(6) Hänggi, P.; Talkner, P.; Borkovec, M. *Rev. Mod. Phys.* **1990**, *62*, 251, and references therein.
(7) Tucker, S. C.; Tuckerman, M. E.; Berne, B. J.; Pollak, E. *J. Chem. Phys.* **1991**, *95*, 5809.
(8) Tucker, S. C. *J. Phys. Chem.* **1993**, *97*, 1596.
(9) Pollak, E. In *Dynamics of Molecules and Chemical Reactions*; Wyatt, R. E., Zhang, J., Eds.; Marcel Dekker: New York, 1996.
(10) Zwanzig, R. *J. Chem. Phys.* **1960**, *33*, 1338.
(11) Zwanzig, R. In *Lectures in Theoretical Physics (Boulder)*; Brittin, W. E., Downs, B. W., Downs, J., Eds.; Wiley-Interscience: New York, 1961; Vol. 3.
(12) Prigogine, J.; Resibois, P. *Physica* **1961**, *27*, 629.
(13) Ford, G. W.; Kac, M.; Mazur, P. *J. Math. Phys.* **1965**, *6*, 504.
(14) Mori, H. *Prog. Theor. Phys.* **1965**, *33*, 423.
(15) Oxtoby, D. W. *Annu. Rev. Phys. Chem.* **1981**, *32*, 77.
(16) Huston, S. E.; Rossky, P. J.; Zichi, D. A. *J. Am. Chem. Soc.* **1989**, *111*, 5680.
(17) Rossky, P. J.; Simon, J. D. *Nature* **1994**, *370*, 263.
(18) Skinner, J. L. *Annu. Rev. Phys. Chem.* **1988**, *39*, 463.
(19) Hernandez, R.; Somer, F. L. *J. Phys. Chem. B* **1999**, *103*, 1064.
(20) Hernandez, R.; Somer, F. L. *J. Phys. Chem. B* **1999**, *103*, 1070.
(21) Andersen, H. C. *J. Chem. Phys.* **1980**, *72*, 2384.
(22) Nosé, S. *J. Chem. Phys.* **1984**, *81*, 511.
(23) Nosé, S. *Mol. Phys.* **1984**, *52*, 255.
(24) Hoover, W. G. *Phys. Rev. A* **1985**, *31*, 1695.
(25) Hoover, W. G. *Phys. Rev. A* **1986**, *34*, 2499.
(26) Martyna, G. J.; Klein, M. L.; Tuckerman, M. *J. Chem. Phys.* **1992**, *97*, 2635.
(27) Hernandez, R., *J. Chem. Phys.* **1999**, *110*, 7701.
(28) Hoover, W. G.; Posch, H. A. *Phys. Let. A* **1998**, *246*, 247.

(29) van Blaaderen, A.; Wiltzius, P. *Science* **1995**, *270*, 1177.
(30) Zahorchak, J. C.; Kurnikova, M. G.; Coalson, R. D. *J. Chem. Phys.* **1997**, *106*, 1585.
(31) Lucchese, R. R.; Tully, J. C. *J. Chem. Phys.* **1984**, *81*, 6313.
(32) Stinnett, J. A.; Madix, R. J.; Tully, J. C. *J. Chem. Phys.* **1996**, *104*, 3134.
(33) Kubo, R. *Rep. Prog. Theor. Phys.* **1966**, *29*, 255.
(34) Zwanzig, R.; Bixon, M. *Phys. Rev. A* **1970**, *2*, 2005.
(35) Metiu, H.; Oxtoby, D.; Freed, K. F. *Phys. Rev. A* **1977**, *15*, 361.
(36) Straub, J. E.; Borkovec, M.; Berne, B. J. *J. Chem. Phys.* **1985**, *83*, 3172.
(37) Straub, J. E.; Borkovec, M.; Berne, B. J. *J. Chem. Phys.* **1986**, *84*, 1788.
(38) Tucker, S. C. *J. Chem. Phys.* **1994**, *101*, 2006.
(39) Press, W. H.; Flannery, B. P.; Teukolsy, S. A.; Vetterling, W. T. *Numerical Recipes*; Cambridge University Press: Cambridge, UK, 1988.